Dysregulation of Ca$_v$1.4 channels disrupts the maturation of photoreceptor synaptic ribbons in congenital stationary night blindness type 2

Xiaoni Liu[1,2], Vasily Kerov[1,2,3], Françoise Haeseleer,[4] Anurima Majumder[1,] Nikolai Artemyev[1], Sheila A Baker[3], and Amy Lee[1,2,]*

[1]Department of Molecular Physiology and Biophysics; University of Iowa; Iowa City, IA USA; [2]Departments of Otolaryngology-Head and Neck Surgery, and Neurology; University of Iowa; Iowa City, IA USA; [3]Department of Biochemistry; University of Iowa; Iowa City, IA USA; [4]Department of Physiology and Biophysics; University of Washington; Seattle, WA USA

Mutations in the gene encoding Ca$_v$1.4, *CACNA1F* are associated with visual disorders including X-linked incomplete congenital stationary night blindness type 2 (CSNB2). In mice lacking Ca$_v$1.4 channels, there are defects in the development of "ribbon" synapses formed between photoreceptors (PRs) and second-order neurons. However, many CSNB2 mutations disrupt the function rather than expression of Ca$_v$1.4 channels. Whether defects in PR synapse development due to altered Ca$_v$1.4 function are common features contributing to the pathogenesis of CSNB2 is unknown. To resolve this issue, we profiled changes in the subcellular distribution of Ca$_v$1.4 channels and synapse morphology during development in wild-type (WT) mice and mouse models of CSNB2. Using Ca$_v$1.4-selective antibodies, we found that Ca$_v$1.4 channels associate with ribbon precursors early in development and are concentrated at both rod and cone PR synapses in the mature retina. In mouse models of CSNB2 in which the voltage-dependence of Ca$_v$1.4 activation is either enhanced (Ca$_v$1.4$_{I756T}$) or inhibited (CaBP4 KO), the initial stages of PR synaptic ribbon formation are largely unaffected. However, after postnatal day 13, many PR ribbons retain the immature morphology. This synaptic abnormality corresponds in severity to the defect in synaptic transmission in the adult mutant mice, suggesting that lack of sufficient mature synapses contributes to vision impairment in Ca$_v$1.4$_{I756T}$ and CaBP4 KO mice. Our results demonstrate the importance of proper Ca$_v$1.4 function for efficient PR synapse maturation, and that dysregulation of Ca$_v$1.4 channels in CSNB2 may have synaptopathic consequences.

Introduction

In the retina, light-dependent changes in the photoreceptor (PR) membrane potential modulate the opening of presynaptic voltage-gated Ca$_v$1 (L-type) Ca^{2+} channels—a process that shapes Ca^{2+}-dependent exocytosis of glutamate at the first synapse in the visual pathway. Of multiple classes of Ca$_v$1 channels (Ca$_v$1.1–1.4), Ca$_v$1.4 is thought to be the major Ca$_v$ channel at PR synapses. More than 50 mutations in the *CACNA1F* gene encoding the pore-forming α$_1$ subunit of Ca$_v$1.4 are linked to multiple visual disorders including incomplete congenital stationary night blindness type 2 (CSNB2).[1] The visual phenotypes associated with CSNB2 are heterogeneous and may include abnormal visual acuity, night blindness, myopia, and/or nystagmus.[2]

Despite strongly reduced transmission by rod and/or cone PRs, vision impairment is relatively modest in CSNB2 patients.[3-5] It has been suggested that Ca$_v$1.4 may not predominate at cone PR synapses,[6] which is at odds with the lack of cone and rod PR synaptic transmission in Ca$_v$1.4 knockout (KO) mice.[7] A

confounding factor is that in addition to their role in regulating PR synaptic transmission, Ca$_v$1.4 channels are required for the development of both rod and cone PR synapses in the mouse.[8,9] The mature "ribbon" structure that is specialized for high-throughput and tonic exocytosis[10] is absent in Ca$_v$1.4 KO mice,[8,9] which may contribute to the complete absence of retinal output in these mice.[7] It is not known if CSNB2-associated mutations that alter the function rather than the expression of Ca$_v$1.4 channels similarly affect PR synapses.

In the mouse retina, rod PR synaptogenesis occurs postnatally and involves formation of dyadic synapses between PRs and horizontal cell dendrites around postnatal day 8 (P8); invagination of postsynaptic bipolar dendrites after eye opening (~P13) completes maturation of the PR synaptic triad.[11] A hallmark of PR synapse development is the assembly of the ribbon, which originates as small round spheres that gradually take on the horseshoe-shaped morphology of the mature synapse.[12] Presynaptic abnormalities have been evaluated only after P10 in Ca$_v$1.4 KO mice,[8,9] so whether Ca$_v$1.4 channels are required for synapse formation and/or maintenance is unknown. Moreover,
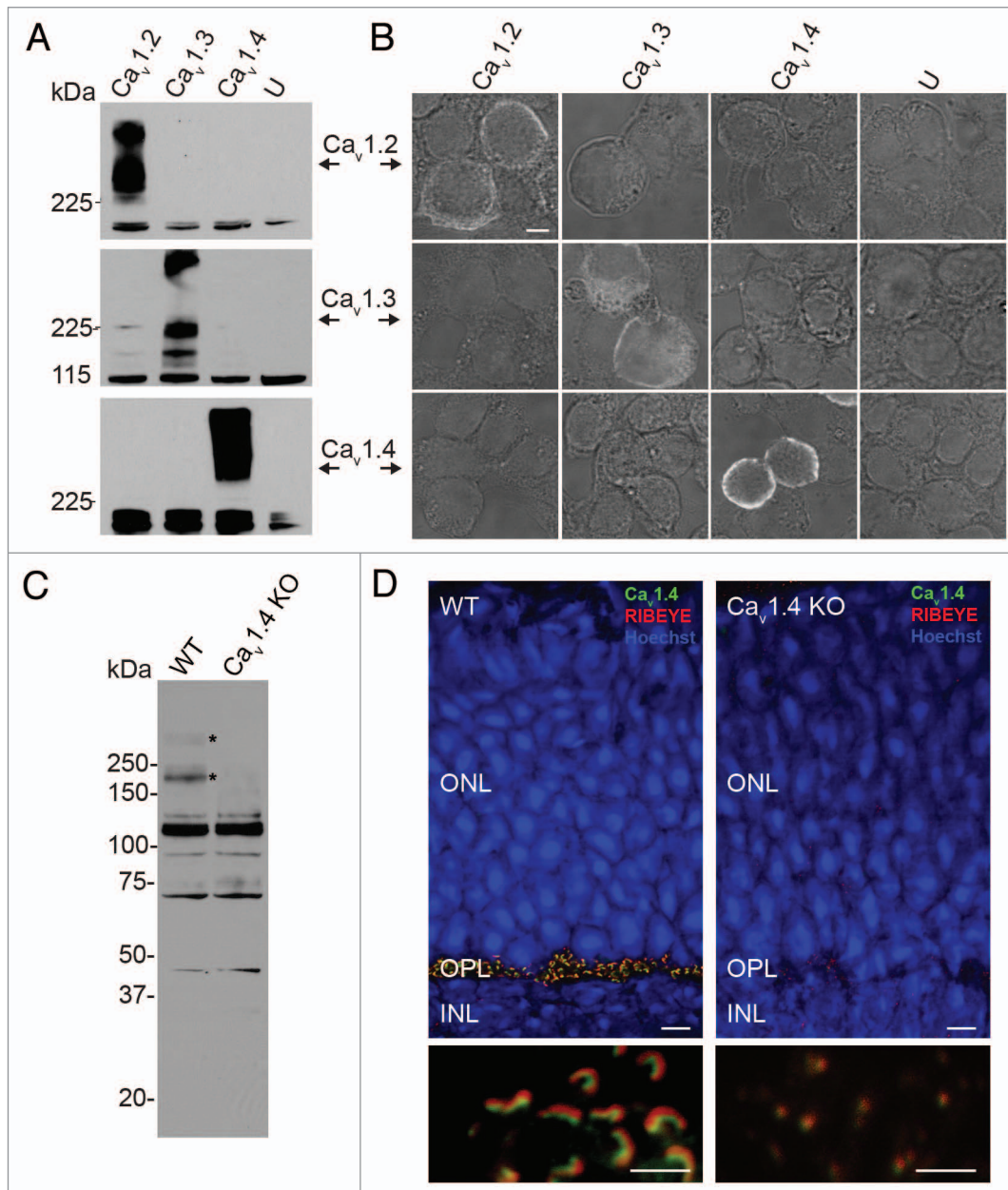
Figure 1. Rabbit polyclonal antibodies specifically recognize $Ca_v1.4$ in transfected cells and in mouse retina. (**A and B**) western blot (**A**) and immunofluorescence (**B**) of HEK293T cells that were untransfected (U) or transfected with $Ca_v1.2$, $Ca_v1.3$, or $Ca_v1.4$. In (**A and B**), antibodies against $Ca_v1.2$ (top panels), $Ca_v1.3$ (middle panels), or $Ca_v1.4$ (bottom panels) were used. (**C**) Western blot of retinal lysate from WT and $Ca_v1.4$ KO mice (50 µg protein/lane) probed with $Ca_v1.4$ antibodies. Astericks indicate proteins present in WT but not $Ca_v1.4$ KO retina. (**D**) Immunofluorescent labeling with $Ca_v1.4$ and RIBEYE antibodies in retina from WT and $Ca_v1.4$ KO mice. Nuclei are stained with Hoechst. Lower panels show high magnification images of double-labeling in the outer plexiform layer (OPL). ONL, outer nuclear layer; INL, inner nuclear layer. Scale bars: 2 µm (**B**); 10 µm, (**D**, upper panels); 2 µm (**D**, lower panels). Results shown are representative of at least 3 independent experiments.

it is not clear if alterations in PR synapse development are common features of CSNB2 that can contribute to the pathogenic mechanisms.

To clarify these ambiguities, we defined the subcellular localization of $Ca_v1.4$ in the developing and mature retina, and compared the development of PR synaptic ribbons in WT mice and in mouse models of CSNB2 in which the voltage-dependence of activation of $Ca_v1.4$ is either enhanced or inhibited. Our findings indicate that $Ca_v1.4$ channels are positioned at the developing and mature active zone of PR synapses, where their presence is required for the initial stages of ribbon assembly. Moreover, the proper function of $Ca_v1.4$ channels is required for the efficient maturation of the synaptic ribbon, which is functionally disrupted in different mouse models of CSNB2.

Figure 2. Ca$_v$1.4 antibodies label cone PR synapses. Double-labeling with antibodies against Ca$_v$1.4 (green) and PNA (red) in retina from mouse (**A**), macaque (**B**), and human (**C**). In (**A and B**), arrows and arrowheads indicate localization of PNA and Ca$_v$1.4, respectively, at elongated structures resembling cone synapses. In (**C**), arrowheads indicate Ca$_v$1.4 labeling clustered at PNA-labeled cone synapses. Inset in (**C**) shows high magnification view of boxed region. Scale bars: 2 μm. Results in (**A**) are representative of at least 3 independent experiments. Results in (**B and C**) are from 1 experiment.

Results

Polyclonal antibodies are selective for Ca$_v$1.4 and report the localization of the channel at rod and cone PR synapses in the retina

To characterize the subcellular localization of Ca$_v$1.4 during development in the mouse retina, we generated polyclonal antibodies against the cytoplasmic N-terminal domain of the Ca$_v$1.4 α$_1$ subunit. Since both Ca$_v$1.3 and Ca$_v$1.2 are thought to be expressed in cone PRs[13] and bipolar neurons,[14] respectively, we confirmed that the antibodies detected Ca$_v$1.4, but not Ca$_v$1.2 or Ca$_v$1.3, by western blot and immunofluorescence of transfected HEK293T cells (**Fig. 1A** and **B**). To determine the specificity of the antibodies for detecting Ca$_v$1.4 in the retina, we performed western blotting of retinal lysates from wild-type (WT) mice and mice lacking expression of functional Ca$_v$1.4 channels (Ca$_v$1.4 KO) due to excision of exons 14 to 17 of the mouse *CACNA1F* gene.[15] In lysate from WT but not Ca$_v$1.4 KO retina (**Fig. 1C**), the antibodies detected a ~200–250 kDa protein that corresponded to the predicted molecular weight of the Ca$_v$1.4 α$_1$ subunit. A protein of higher molecular weight was also detected, which may reflect the reduced electrophoretic mobility of aggregated Ca$_v$1.4 protein upon denaturation, as such high-molecular bands were also detected in HEK293T cells transfected with Ca$_v$1.4 (**Fig. 1A**). Additional lower-molecular weight proteins were also detected, but were considered non-specific in that they were seen in both genotypes.

By immunofluorescence of WT mice, Ca$_v$1.4 antibodies labeled numerous horseshoe-shaped structures in the outer plexiform layer (OPL), which contains mostly rod PR terminals (spherules) in the mouse retina (**Fig. 1D**). These structures were also labeled with antibodies against RIBEYE, the major component of the ribbon,[16] and resembled synapses formed between a single rod spherule and dendrites of bipolar neurons and horizontal
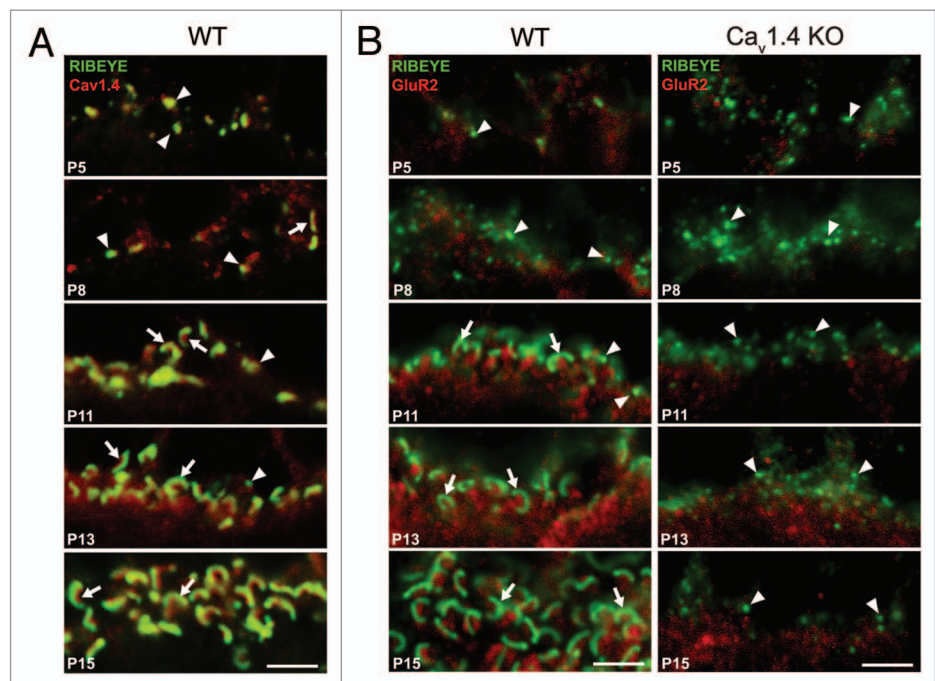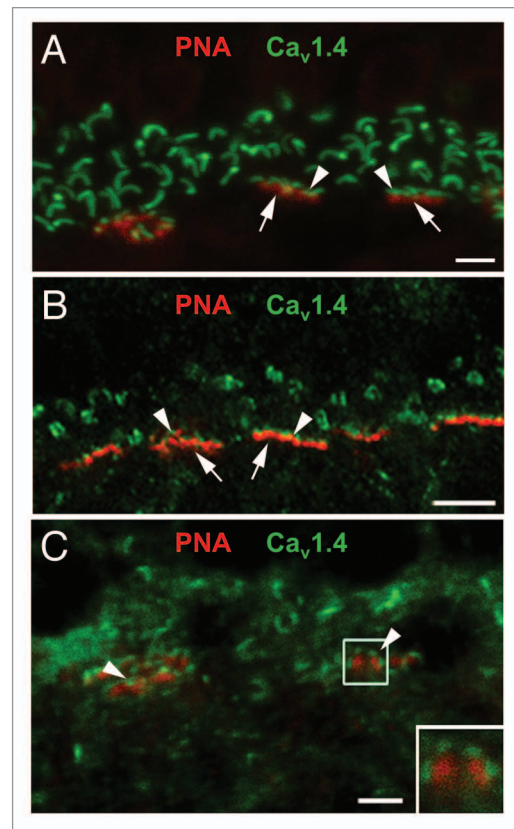

Figure 3. Ca$_v$1.4 is required for synapse formation. (**A**) Immunofluorescence for RIBEYE (green) and Ca$_v$1.4 (red) in retina from WT mice (P5-P15). (**B**) Immunofluorescence for RIBEYE (green) and GluR2 in retina from WT (left) and Ca$_v$1.4 KO (right) mice (P5-P15). Mature (arrows) and immature (arrowheads) ribbon morphologies are indicated. Scale bars: 2 μm. Results shown are representative of at least 3 independent experiments.
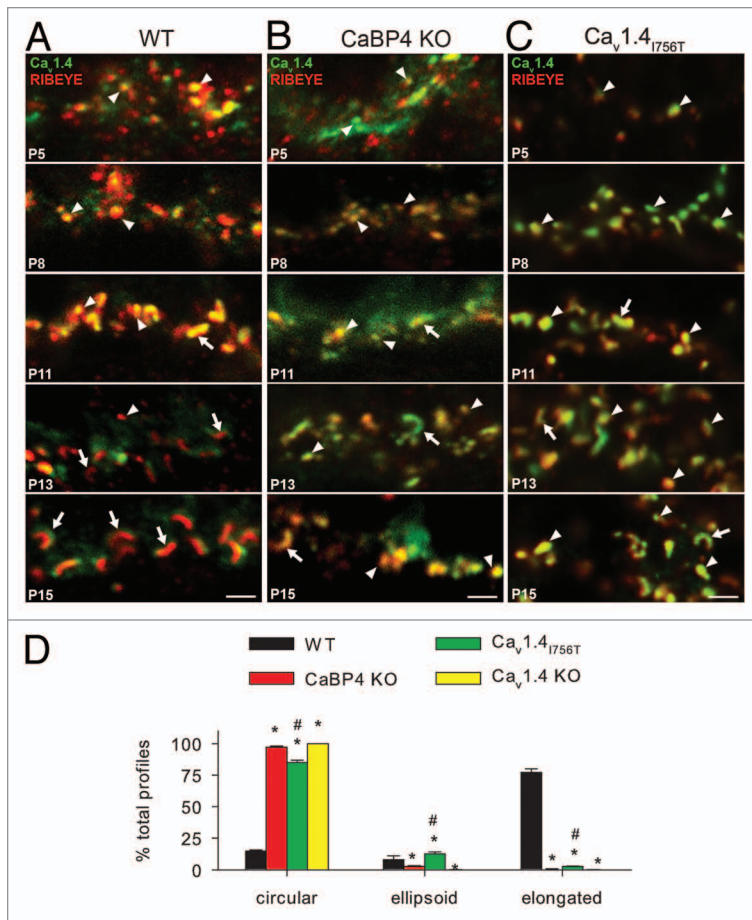
Figure 4. The maturation of synaptic ribbons is impaired in CaBP4 KO and Ca$_v$1.4$_{I756T}$ mouse retina. (**A–C**) Immunofluorescence for RIBEYE (red) and Ca$_v$1.4 (green) in retina from WT (**A**), CaBP4 KO (**B**), and Ca$_v$1.4$_{I756T}$ (**C**) mice (P5-P15). Mature (arrows) and immature (arrowheads) ribbon morphologies are indicated. Scale bars: 2 μm. (**D**) Quantitative analysis of ribbon morphologies in retinal sections that were single-labeled with RIBEYE antibodies. RIBEYE-positive profiles were categorized according to morphology as described in the Materials and Methods and presented as the mean ± SEM. The total number of profiles examined was 1003 (WT), 1073 (Ca$_v$1.4$_{I756T}$), 1140 (CaBP4 KO), and 1118 (Ca$_v$1.4 KO) in 5 animals per genotype; the retinas from each were processed in independent experiments. *, p < 0.001 compared with WT by ANOVA; #, p < 0.05 compared with CaBP4 KO by Student Newman-Keuls test.

Mature rod PR synapses fail to form in Ca$_v$1.4 KO mice

Using these Ca$_v$1.4-selective antibodies, we profiled the distribution of Ca$_v$1.4 at developing PR synapses from P5-P15 in the mouse retina. From P5-P8, labeling for Ca$_v$1.4 and RIBEYE was largely colocalized in small puncta resembling ribbon precursor spheres[11,12] in the OPL (**Fig. 3A**). Between P11-P15, Ca$_v$1.4-labeled ribbons become more elongated, and depending on the plane of section, take on the horseshoe-shaped morphology of mature rod PR synapses (**Fig. 3A**).[11] The temporal and spatial coincidence of Ca$_v$1.4 and RIBEYE labeling in the OPL is consistent with a role for Ca$_v$1.4 channels in directing PR synapse assembly.

To determine if the synaptic defects in Ca$_v$1.4 KO mice[7,9,15] result from alterations in PR synapse formation or maintenance, we double-labeled with antibodies against RIBEYE and a glutamate receptor (GluR2) expressed in postsynaptic horizontal cell dendrites.[18] In the OPL of WT retina, morphologically mature synapses are seen as early as P11 and predominate at P15 (**Fig. 3B**). In Ca$_v$1.4 KO retina, mature ribbons were not found; only RIBEYE-positive spheres were present, none of which were associated with GluR2-labeling at any age that was examined (**Fig. 3B**). The amount of RIBEYE labeling declines slightly beginning at P15 and is most apparent in adult Ca$_v$1.4 KO mice (compare **Figs. 3B** and **1D**). These results demonstrate that Ca$_v$1.4 channels are required for the initial formation of PR synapses.

PR synapse maturation is impaired in mouse models of CSNB2

CaBP4 is a Ca^{2+} binding protein that interacts with, and enhances voltage-dependent activation of, Ca$_v$1.4 channels.[19,20] Electroretinograms (ERGs) of CaBP4 KO mice indicate a loss of both rod and cone PR synaptic transmission,[19,21] consistent with reduced function of Ca$_v$1.4 channels and the CSNB2-like phenotypes associated with human mutations in the *Cabp4* gene.[5,22,23] PR synapses are morphologically abnormal in CaBP4 KO mice,[19] which may be due to aberrant ribbon synapse assembly and/or maturation. To probe the underlying mechanism, we analyzed developmental changes in PR ribbon morphologies in WT and CaBP4 KO mice. Compared with age-matched WT control retina, ribbons were similar in CaBP4 KO retina through P13 (**Fig. 4A** and **B**). At this age, a number of elongated and horseshoe-shaped ribbons were seen in both genotypes, which indicated no deficits in the initial stages of synapse assembly. However at P15, when all ribbons take on elongated and horseshoe-shaped morphologies in WT retina, RIBEYE-positive structures that were small and round outnumbered those resembling mature ribbons in CaBP4 KO retina (**Fig. 4A** and **B**). Double-labeling with Ca$_v$1.4 antibodies revealed the association of Ca$_v$1.4 channels with both normal and abnormal ribbons, which indicated that alterations in ribbon structure did not result from failures in Ca$_v$1.4 expression or trafficking to synapses. These findings supported a requirement for
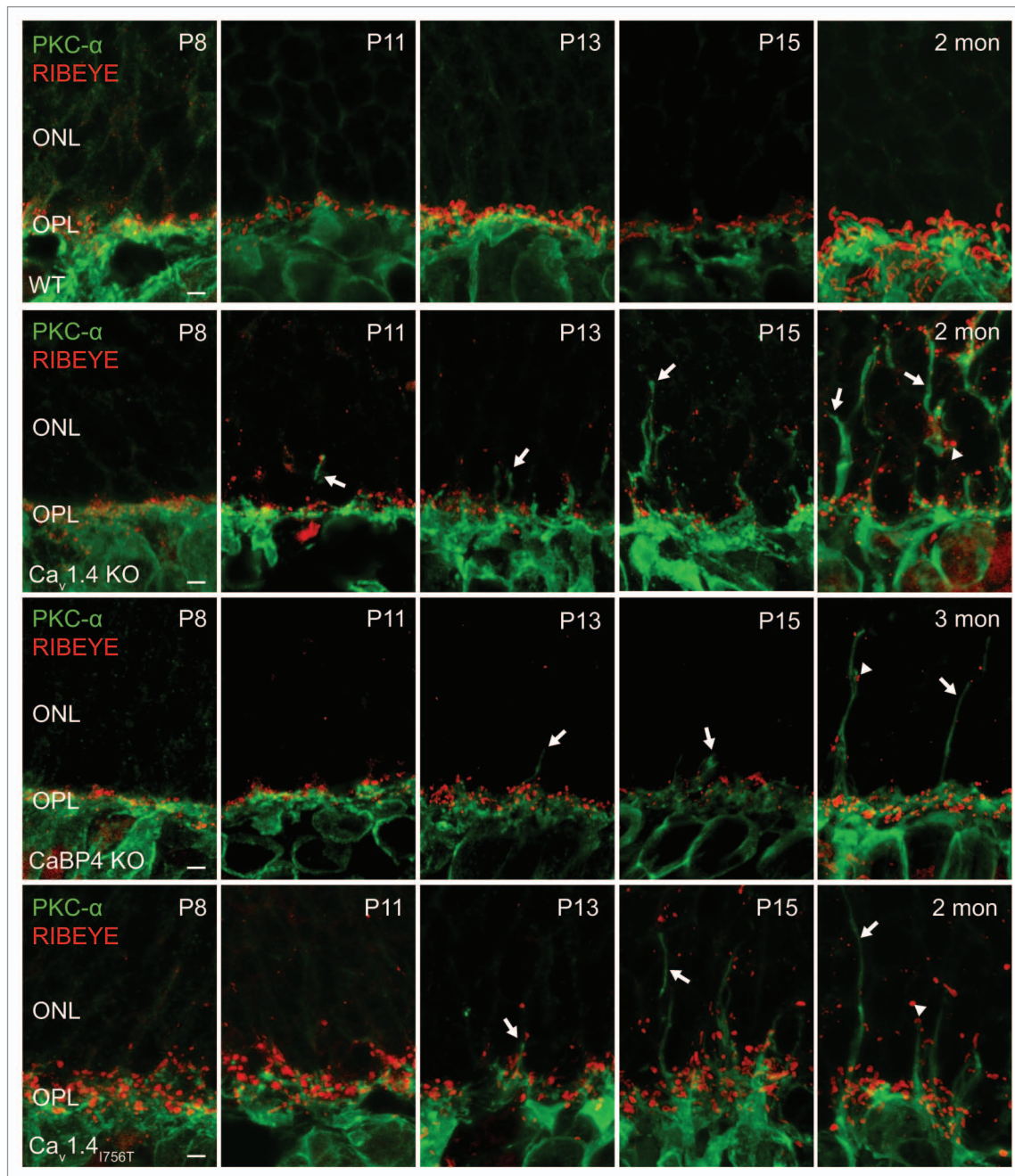
cells.[11] As in previous reports that used different Ca$_v$1.4 antibodies,[15] Ca$_v$1.4 labeling was slightly shifted compared with that for RIBEYE (**Fig. 1D**), consistent with the localization of Ca$_v$1.4 at the arciform density, a subsynaptic structure adjacent to the ribbon.[10,17] This pattern of labeling was absent in the OPL of Ca$_v$1.4 KO retina (**Fig. 1D**). Using fluorescently tagged peanut agglutinin (PNA) to label cones, we also observed Ca$_v$1.4 labeling in cone terminals (pedicles) in mouse retina (**Fig. 2A**). In macaque and human retinas, Ca$_v$1.4 antibody labeling closely aligned with that for PNA, and was associated with horseshoe-shaped structures resembling rod synapses throughout the OPL (**Fig. 2B** and **C**). Taken together, these results confirm the specificity of our antibodies, and show that Ca$_v$1.4 channels are localized to both rod and cone PR synapses in the mammalian retina.

Figure 5. Postsynaptic remodeling and ectopic ribbons in mice with altered $Ca_v1.4$ function. Double-label immunofluorescence of PKCα (green) and RIBEYE (red) in retina from WT, $Ca_v1.4$ KO, CaBP4 KO, or $Ca_v1.4_{I756T}$ mice (P8-adult). In WT retina, bipolar dendrites labeled with PKCα antibodies ramify in the OPL where they form synapses with rod spherules. In $Ca_v1.4$ KO mice, bipolar dendrites (arrows) start extending into the outer nuclear layer (ONL) at P11, and ectopic ribbons labeled by RIBEYE antibodies are evident (arrowheads). Postsynaptic remodeling emerges later in CaBP4 KO and $Ca_v1.4_{I756T}$ mice (~P13), and is less severe in adulthood (2-mo old) compared with WT mice. Scale bars: 2 μm. Results shown are representative of at least 3 independent experiments.

CaBP4, perhaps via regulation of $Ca_v1.4$ channels, in the maturation of rod PR ribbons.

To confirm the importance of proper $Ca_v1.4$ function for ribbon synapse development, we utilized knock-in mice harboring a mutation that causes CSNB2 in humans ($Ca_v1.4_{I756T}$). This mutation (I745T in the human *CACNA1F* gene) results in a large negative shift in the voltage-dependence of channel activation,[24] and so should potentiate $Ca_v1.4$ function, in contrast to the inhibition of $Ca_v1.4$ that would be expected in CaBP4 KO mice. As in CaBP4 KO mice, the pattern of RIBEYE/$Ca_v1.4$ labeling was similar in WT and $Ca_v1.4_{I756T}$ mice through P13, but diverged at P15, with many ribbons exhibiting the immature morphology in the mutant but not the WT mice (**Fig. 4A** and **C**). Thus, both the loss – and gain – of
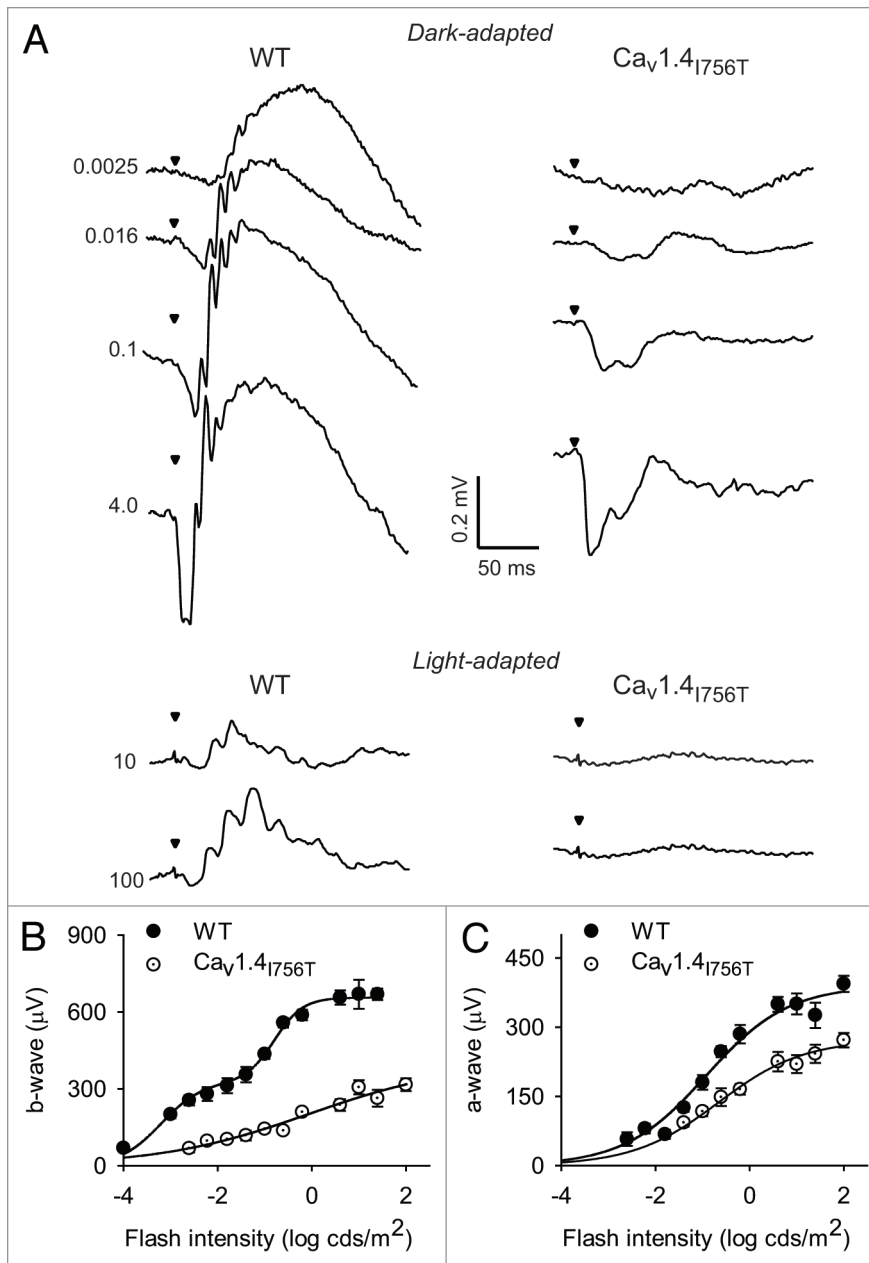
Figure 6. ERGs from WT and $Ca_v1.4_{I756T}$ mice. (**A**) Representative voltage traces from flash ERG recordings in 5–6-week old dark – adapted or light-adapted WT and $Ca_v1.4_{I756T}$ mice. Arrowheads indicate time of flash, numbers indicate flash intensities (cd·s /m²). (**B** and **C**) b-wave amplitudes (**B**) and a-wave amplitudes (**C**) measured from recordings of dark-adapted mice obtained as in (**A**). Points represent the mean ± SEM (n = 8; left and right eyes from 4 mice). Smooth lines represent fits from double (WT in **B**) or single sigmoidal functions.

the plane of section. Indeed, a minor fraction of RIBEYE labeling in WT mice was associated with circular (14.8 ± 0.94%) or ellipsoid (8.0 ± 2.9%) profiles. Unlike in WT mice, circular profiles accounted for most of the RIBEYE labeling in CaBP4 KO (97.0 ± 0.9%) and $Ca_v1.4_{I756T}$ (84.9 ± 0.2%) (**Fig. 4D**). Notably, the proportion of elongated and ellipsoid profiles was significantly greater (p < 0.001 by ANOVA) in $Ca_v1.4_{I756T}$ (2.6 ± 0.5% elongated, 12.6 ± 1.5% ellipsoid) than in CaBP4 KO (0.4 ± 0.3% elongated, 2.6 ± 0.7% ellipsoid; p < 0.001 by ANOVA) mice (**Fig. 4D**). Taken together, these results suggested a defect in PR ribbons of the following rank order in severity: $Ca_v1.4$ KO ≥ CaBP4 KO > $Ca_v1.4_{I756T}$ (**Fig. 4D**).

Structural remodeling of horizontal and bipolar cell dendrites and the formation of ectopic synapses in the outer nuclear layer (ONL) are common features of mice with PR synapse defects.[25] If postsynaptic modeling results from altered PR ribbon maturation in CaBP4 KO and $Ca_v1.4_{I756T}$ mice, it should be evident between P13 and P15, when presynaptic defects in these mice are first apparent (**Fig. 4B** and **C**). To test this, we analyzed retinas from P8 to adulthood that were double-labeled with RIBEYE and PKCα, a marker for rod bipolar cells. As shown previously,[7,19] bipolar dendrites extending into the ONL were found in adult retina of $Ca_v1.4$ KO and CaBP4 KO mice. RIBEYE-labeled puncta were associated with these processes, suggestive of ectopic ribbon synapses (**Fig. 5**). This pattern of labeling emerged earlier in $Ca_v1.4$ KO (~P11) than in CaBP4 KO and $Ca_v1.4_{I756T}$ retinas (~P13, **Fig. 5**), consistent with the more severe presynaptic defects in the $Ca_v1.4$ KO mice (**Figs. 3B** and **4D**).

To determine if the impaired ribbon maturation in the mutant mice corresponded to deficits in PR synaptic transmission, we performed ERG analyses, which monitor light-induced changes in the electrical activity of presynaptic PRs (a-wave) and postsynaptic second-order neurons (b-waves) (**Fig. 6A**). Previous ERG analyses established strongly reduced b-waves in CaBP4 KO mice under dark-adapted conditions to measure rod PR transmission.[19] Therefore, we restricted analyses to comparisons of $Ca_v1.4_{I756T}$ mice with WT mice. Due to the presence of rod – and cone-driven responses in WT mice, plots of b-wave amplitudes against flash intensity were fit with a double-sigmoidal function (**Fig. 6B**). In contrast, the corresponding data in $Ca_v1.4_{I756T}$ mice were described by a single sigmoidal fit (**Fig. 6B**). Since ERG recordings under light-adapted conditions indicated that $Ca_v1.4_{I756T}$

function in $Ca_v1.4$ channel properties can impair PR ribbon development in the mouse retina.

To quantitate the severity of the synaptic defects in the various adult mutant mice, we compared the distribution of RIBEYE-labeled profiles as either circular, ellipsoid, or elongated. We assumed that circular profiles generally represent immature ribbon precursors, as nearly all (99.8 ± 0.1%) RIBEYE-positive structures were circular in $Ca_v1.4$ KO retina (**Fig. 4D**). However, some mature elongated ribbons could appear circular or ellipsoid, depending on

mice lack cone-driven responses (**Fig. 6A**), we assumed that the b-wave responses from dark-adapted $Ca_v1.4_{I756T}$ mice are largely due to rod transmission. Compared with rod-driven responses in WT mice, b-waves were significantly reduced, although not abolished, in $Ca_v1.4_{I756T}$ mice (~66–74% compared with WT, at light intensities (I) < − 1.0 log cd•s/m², p < 0.001 by ANOVA; **Fig. 6B**). In addition, the sensitivity of rod-rod bipolar synaptic transmission in $Ca_v1.4_{I756T}$ mice ($I_{1/2}$) was significantly reduced ($I_{1/2} = − 3.2 ± 0.2$ log cd•s /m² for WT vs. − 0.3 ± 0.6 log cd s /m² for I_{756T}; p < 0.001 by t-test). While the maximal a-wave amplitudes appeared to be reduced in $Ca_v1.4_{I756T}$, the difference with WT was not significant (385.3 ± 14.2 for WT vs. 301.3 ± 48.2 for $Ca_v1.4_{I756T}$; p = 0.1 by t-test, **Fig. 6C**). There was also no significant difference in the flash intensities evoking the half-maximal a-wave response ($I_{1/2} = −$ 0.9 ± 0.1 for WT vs. − 0.5 ± 0.4 log cd•s/m² for $Ca_v1.4_{I756T}$; p = 0.2 by t-test). These results argued against the possibility that deficient b-wave responses in dark-adapted $Ca_v1.4_{I756T}$ mice were due to decreased sensitivity or changes in the numbers of functional rod PRs. Moreover, at light intensities at which the a-waves were nearly identical in dark-adapted WT and $Ca_v1.4_{I756T}$ mice (e.g., I < − 1 log cd•s/m²), the b-wave was still significantly smaller in the latter (p < 0.001 by ANOVA; **Fig. 6B** and **C**). Taken together, these results strongly supported a major defect in PR transmission in $Ca_v1.4_{I756T}$ mice. The less severe rod-driven responses in $Ca_v1.4_{I756T}$ mice compared with CaBP4 KO and $Ca_v1.4$ KO mice[7,19] are consistent with the more moderate abnormalities in ribbon maturation in the former compared with the latter 2 mice (**Figs. 4** and **5**). Our results support a requirement for normal $Ca_v1.4$ function in the maturation of rod PR synaptic ribbons, which may impact the efficacy of synaptic transmission in the adult mice.

Discussion

Localization of $Ca_v1.4$ at rod and cone PR synapses

Due to the notorious non-specificity of Ca_v channel antibodies, we rigorously characterized the $Ca_v1.4$ antibodies that we generated and used in this study (**Fig. 1**). While other antibodies generated against $Ca_v1.4$ were shown to label rod PR synapses,[7,15] our study is the first to document the localization of $Ca_v1.4$ in cone PR synapses (**Fig. 2**). Cones comprise < 3% of the PRs in the rodent retina,[26,27] which may explain the difficulties in detecting $Ca_v1.4$ colocalization with markers of cone PR synapses in the rat.[28] $Ca_v1.3$ expression has been reported in cone PRs in mouse and tree shrew retinas,[6,29] and modest morphological changes in PR ribbon morphology have been reported in mice lacking $Ca_v1.3$.[30] However, we propose that $Ca_v1.4$ channels are functionally the dominant Ca_v channels in cone PRs for the following reasons. First, we found strong labeling of cone PR terminals in multiple species (**Fig. 2**). Second, mice lacking $Ca_v1.4$ but not $Ca_v1.3$ expression exhibit severe defects in cone-mediated visual responses,[7,31] and a loss-of function mutation in the *CACNA1D* gene encoding $Ca_v1.3$ channels, causes cardiac arrhythmia and deafness, but no major visual deficits.[30,32] In contrast, a number of mutations in *CACNA1F* including the human I745T mutation,[33] produce severe defects in cone and rod responses in humans.[34,35] Therefore, $Ca_v1.4$ channels likely

play an analogous role in regulating exocytosis at cone and rod PRs.

A dual role for $Ca_v1.4$ in PR ribbon assembly

The stages involved in the molecular and morphological development of PR ribbon synapses have been elegantly described.[11,12,17] Prior to P10, ribbon precursor spheres complete their molecular assembly with the addition of ribbon-associated proteins (e.g., RIBEYE, bassoon, and piccolo) and proteins of the arciform density (e.g., RIM2, munc13, $Ca_v1.4$). Between P10 and P14, ribbons are largely mature at the molecular level, but make the final morphological transition and become anchored to the plasma membrane.[12] The observation that PR ribbons develop normally through P13 in CaBP4 KO and $Ca_v1.4_{I756T}$ mice (**Fig. 4**), but not in $Ca_v1.4$ KO mice (**Fig. 3B**), indicates that the maturation but not the initial assembly of the ribbon depends on the proper activation properties of the $Ca_v1.4$ channel.

Initially, $Ca_v1.4$ channels may be required to scaffold key presynaptic proteins such as PSD-95 and the plasma membrane Ca^{2+} ATPase, both of which are absent in developing PR terminals of $Ca_v1.4$-deficient mice.[8,36] At this stage, $Ca_v1.4$ channels are clustered in RIBEYE-positive puncta that likely represent immature ribbon precursors (**Fig. 3A**),[12] and so may not be positioned at the presynaptic membrane where their Ca^{2+} conducting function may be required. Upon eye-opening at P13, light-modulated changes in $Ca_v1.4$ opening may shape presynaptic Ca^{2+} signals and exocytosis which support efficient PR synapse maturation. These Ca^{2+} signals would be strongly reduced in CaBP4 KO mice, since there would be limited activation of $Ca_v1.4$ channels at the PR membrane potential in darkness (~-40 mV) in the absence of CaBP4.[19] In $Ca_v1.4_{I756T}$ mice, presynaptic Ca^{2+} influx in darkness should be abnormally elevated due to a ~-30 mV shift in the voltage-dependence of activation, and slower voltage-dependent inactivation, caused by this mutation.[24] The more severe morphological and functional defects in PR synapses in CaBP4 KO compared with $Ca_v1.4_{I756T}$ mice (**Figs. 4** and **6**)[19] may reflect greater synaptic consequences of the loss-of function compared with the gain-of function of $Ca_v1.4$, although we cannot discount the possibility that CaBP4 may have effects independent of $Ca_v1.4$ on promoting ribbon maturation. While our immunocytochemical data indicated no major differences in the intensity of $Ca_v1.4$ labeling at PR synapses in CaBP4 KO and $Ca_v1.4_{I756T}$ mice at P15 (**Fig. 4**), we cannot rule out that there may be a progressive reduction in levels of $Ca_v1.4$ channels, which could contribute to the visual impairment measured in these mice at later ages (**Fig. 6** and in Haeseleer et al.[19]). Ca_v1 channels may play a general role in the development of ribbon synapses, since proper function of $Ca_v1.3$ channels has been shown to regulate ribbon size and maintenance at zebrafish hair cell ribbon synapses.[37] Determining the molecular mechanisms by which $Ca_v1.4$ channels promote PR synapse assembly and maturation remains an important challenge for future studies.

Synapthopathic origins of CSNB2

Our findings that most (75–90%) RIBEYE-positive structures exhibited the immature (round) morphology in adult CaBP4 KO and $Ca_v1.4_{I756T}$ mice (**Fig. 4B**) are consistent with the strong reductions in rod PR transmission measured in these mice[19] (**Fig. 6**). Smaller, spherical ribbons are unlikely to support the tethering of

hundreds of synaptic vesicles primed for tonic glutamate release at mature ribbon synapses in darkness.[38] Based on findings that alterations in ribbon structure significantly inhibit rod PR transmission,[39,40] weakened exocytosis at these immature synapses likely contributes to the almost complete absence of rod PR synaptic transmission in $Ca_v1.4$ KO (**Fig. 6B**) and CaBP4 KO[19] mice. The greater preservation of ribbons in $Ca_v1.4_{I756T}$ mice compared with $Ca_v1.4$ KO or CaBP4 KO mice (**Fig. 4D**) may account for the partial sparing of rod PR synaptic transmission in these mice (**Fig. 6B**). Since rod PRs mediate vision in low-light conditions, our findings may help explain the night-blindness phenotype in some patients with loss-of function mutations in *CACNA1F*[1] and *Cabp4*.[5,22] On the other hand, we found that cone-mediated (light-adapted) b-wave responses are absent in $Ca_v1.4_{I756T}$ mice (**Fig. 6A**). Interestingly, patients harboring the analogous I745T mutation[33] as well as some patients with *Cabp4* mutations[23,41] exhibit a more severe loss of vision mediated by cones than by rods. Considering the localization of $Ca_v1.4$ in cone PRs (**Fig. 2**), and previous results that cone PR synaptogenesis is impaired in $Ca_v1.4$ KO mice,[9] we expect that a disruption in cone PR synaptic ribbon maturation may contribute to these visual phenotypes in humans.

Alterations in PR ribbon morphologies and synapses have been reported in mice with reduced or absent expression of $Ca_v1.4$.[7,42] Considering that a number of CSNB2 mutations in *CACNA1F* are predicted to yield dysfunctional channels rather than cause the complete absence of channel expression,[43,44] our findings reveal that alterations in PR synapse development may be a common feature of CSNB2, and that therapeutic interventions for offsetting visual impairment may require early targeting of the synaptopathic consequences of the mutations.

Materials and Methods

Animals

CaBP4 KO[19] and $Ca_v1.4$ KO[15] mice were characterized previously. $Ca_v1.4$ KO (B6.Cg-Cacna1ftm1.1Sdie/J) and $Ca_v1.4_{I756T}$ (B6(Cg)-Cacna1ftm1Sdie/J) were obtained from the Jackson Laboratory. The generation of the $Ca_v1.4$ KO and $Ca_v1.4_{I756T}$ lines was described previously.[15] $Ca_v1.4$ KO mice lack exons 14–17, while $Ca_v1.4_{I756T}$ mice bear a threonine substitution for isoleucine 756, of the mouse *CACNA1F* gene. Male and female mice (5-d – 3 mo old) were used. All animals were maintained on a 12-h light/dark cycle. Experimental procedures using animals were approved by the Institutional Animal Care and Use Committee at the University of Iowa and the University of Washington.

Antibody production and characterization

Polyclonal rabbit $Ca_v1.4$ antibodies were generated against a peptide corresponding to amino acids 1–20 (MSESEVGKDTTPEPSPANGTC) of mouse *CACNA1F* (NP_062528.2) by a commercial source (Covance). Antiserum was subject to affinity purification by standard protocols prior to use.

Immunofluorescence and western blotting of transfected HEK293T cells

Human embryonic kidney (HEK) 293T cells were transfected with cDNAs encoding the α_1 subunit for $Ca_v1.2$, $Ca_v1.3$, $Ca_v1.4$ along with β_{2A} and $\alpha_2\delta$ using GenePORTER transfection reagent (# T201015, Genlantis). After 24 h, transfected cells were processed the next day for immunofluorescence essentially as described previously.[45] Rabbit polyclonal primary antibodies were used at 1:1000 dilution: anti-$Ca_v1.2$,[46] anti-$Ca_v1.3$,[45] anti-$Ca_v1.4$ (this study). Alexa488-conjugated and Alexa568-conjugated secondary antibodies (1:1000; #A11011, Life Technologies) were used. Image analysis was performed using a Fluoview 1000 confocal microscope (Olympus). For western blots, lysates from transfected cells or retina (from 2-mo old mice) were prepared and subjected to SDS-PAGE and western blotting as described.[45] Primary antibodies were the same as those used for immunofluorescence experiments. Secondary detection was with HRP-conjugated anti-rabbit IgG (1:1000; #RPN4301, GE Healthcare) and SuperSignal West Pico Chemiluminescent Substrate (# 34077, Thermo Scientific).

Immunofluorescence of retina

Immunofluorescence processing of the retina was generally as described previously.[19] Macaque retina was obtained at the University of Washington Regional Primate Center and frozen unfixed human retina was obtained from the Iowa Lions Eye Bank (provided by Dr Robert Mullins) following full consent of the donors' next of kin. Mice younger than P10 were killed by decapitation, and mice at P10 or older were anesthetized with isoflurane first and killed by decapitation. Three mice (male or female) per developmental stage were used for each genotype. Mice were allocated to groups according to age or genotype prior to experimentation. Eyes were quickly removed and incubated in 4% paraformaldehyde in 0.1 M phosphate buffer for 10–60 min. The anterior segments were removed, and the posterior eye cups were infiltrated with 30% sucrose on ice and frozen in embedding media on dry ice. Frozen blocks were cut in vertical sections (12 μm) with a cryostat (Leica), collected on electrostatic slides, and stored at – 80 °C until use. Sections were blocked in blocking buffer (3–10% normal goat serum [NGS] and 0.1% Triton X-100 (TX-100) diluted in phosphate-buffered saline [PBS]) overnight at 4 °C. Sections were incubated in primary antibodies for 4 h at room temperature. The following primary antibodies and working dilutions were used: rabbit $Ca_v1.4$ (1:1000), RIBEYE (1: 500–1:1000 #612044, BD bioscience), PKC-α (1:500, #SC208, Santa Cruz, Biotechnology). After rinsing, sections were incubated for 1 h in darkness in secondary antibodies (Life Technologies) used at 1:400 or 1:1000 dilution: Alexa Fluor 488 – goat anti-mouse (#R37120); Alexa 555 – goat anti-rabbit (# A31629); Alexa 488 – goat anti-rabbit (#A11008); Alexa568 – goat anti-mouse (#A11004). All antibodies were diluted in 0.1% TX-100 in PBS and incubations were performed in humidified chambers. In some experiments, Hoechst stain (# H6024, Sigma; 1:1000) was applied for 10 min at room temperature. Between incubations, sections were washed 3 times for 5 min using 0.1% TX-100 in PBS. Sections were coverslipped, sealed with clear nail polish, and stored at 4 °C. Confocal microscopy was performed using an Olympus Fluoview 1000 confocal microscope with 60X or 100X oil-immersion objectives or a Zeiss LSM710 confocal microscope with a Plan-Neofluar 63x/1.4 oil-immersion objective. Previous experience with variabilities in histological techniques was used to determine the number of animals (at least 3 per developmental age per genotype) required

to substantiate conclusions. Samples with poor preservation of tissue morphology, as indicated by transmitted light microscopy or Hoechst staining, were excluded from analysis. For developmental series, processing of tissue from a given mouse strain was done in a single experiment to reduce variability due to differences in experimental conditions. Results shown in all figures are representative of at least 3 independent experiments.

For quantitative analyses of RIBEYE-labeled structures in the adult mouse retina, confocal Z-stack images (5 μm thick) were taken about 1 mm from the optic nerve (2 images/mouse for each of 3 mice per genotype). For elongated structures the length was measured with three segments along the ribbon. Ratios of length to width were calculated and categorized accordingly: spherical (ratio < 2), ellipsoid (2 to 3), elongated (> 3). To reduce experimenter bias, image acquisition and quantitative analyses were done by different researchers in a blinded fashion.

Electroretinography (ERG)

ERG recordings were obtained using the Espion E^3 system (Diagnosys LLC). After overnight dark adaptation, 5- to 6-weeks old mice were prepared for ERG recording under dim red light. Mice (5–6 week old, males and females) were anesthetized by intraperitoneal injection of a ketamine/xylazine mixture (100 and 10 mg/kg, respectively). The pupils were dilated by applying a drop of 1% tropicamide, followed by a drop of 2.5% phenylephrine hydrochloride. ERGs were recorded simultaneously from the corneal surface of each eye using gold ring electrodes (Diagnosys), with a needle electrode placed on the back of the head serving as reference. Another needle electrode placed near the tail served as ground. A drop of Hypromellose 2.5% Ophthalmic Demulcent Solution (# 17478-0064-2, Akorn Gonak) was placed on the corneal surface to ensure electrical contact and to prevent eyes

from drying and cataract formation. Body temperature of mice was maintained at 37°C using the system's heating pad. Mice were placed in a Ganzfeld stimulator chamber (ColorDome; Diagnosys) for delivery of stimuli, and the mouse head and electrode positioning were monitored on the camera attached to the system. ERG responses were evoked in mice by a series of flashes ranging from 0.0001 to 100 cd•s/m^2. Responses to 6 sweeps were averaged for dim flashes up to 0.6 cd•s/m^2, 2 sweeps were averaged for 4 cd·s/m^2, and responses to brighter flashes were recorded without averaging. Intersweep intervals for flashes with increasing strength were increased from 10 to 60 s to allow full recovery from preceding flashes. To record photopic ERGs, mice were exposed to a background light (30 cd•s /m^2) for 3 min before flash stimulation (3, 30, or 100 cd•s/m^2). Six sweeps were averaged. The data were analyzed as described previously[47] using GraphPad Prism software (version 4).

References

1. Lodha N, Loucks CM, Beaulieu C, Parboosingh JS, Bech-Hansen NT. Congenital stationary night blindness: mutation update and clinical variability. Adv Exp Med Biol 2012; 723:371-9; PMID:22183355; http://dx.doi.org/10.1007/978-1-4614-0631-0_48

2. Boycott KM, Pearce WG, Bech-Hansen NT. Clinical variability among patients with incomplete X-linked congenital stationary night blindness and a founder mutation in CACNA1F. Can J Ophthalmol 2000; 35:204-13; PMID:10900517

3. Tremblay F, Laroche RG, De Becker I. The electroretinographic diagnosis of the incomplete form of congenital stationary night blindness. Vision Res 1995; 35:2383-93; PMID:7571473; http://dx.doi.org/10.1016/0042-6989(95)00006-L

4. Miyake Y, Yagasaki K, Horiguchi M, Kawase Y, Kanda T. Congenital stationary night blindness with negative electroretinogram. A new classification. Arch Ophthalmol 1986; 104:1013-20; PMID:3488053; http://dx.doi.org/10.1001/archopht.1986.01050190071042

5. Bijveld MM, Florijn RJ, Bergen AA, van den Born LI, Kamermans M, Prick L, Riemslag FC, van Schooneveld MJ, Kappers AM, van Genderen MM. Genotype and Phenotype of 101 Dutch Patients with Congenital Stationary Night Blindness. Ophthalmology 2013; PMID:23714322; http://dx.doi.org/10.1016/j.ophtha.2013.03.002

6. Morgans CW. Calcium channel heterogeneity among cone photoreceptors in the tree shrew retina. Eur J Neurosci 1999; 11:2989-93; PMID:10457194; http://dx.doi.org/10.1046/j.1460-9568.1999.00719.x

7. Mansergh F, Orton NC, Vessey JP, Lalonde MR, Stell WK, Tremblay F, Barnes S, Rancourt DE, Bech-Hansen NT. Mutation of the calcium channel gene *Cacna1f* disrupts calcium signaling, synaptic transmission and cellular organization in mouse retina. Hum Mol Genet 2005; 14:3035-46; PMID:16155113; http://dx.doi.org/10.1093/hmg/ddi336

8. Zabouri N, Haverkamp S. Calcium channel-dependent molecular maturation of photoreceptor synapses. PLoS One 2013; 8:e63853; PMID:23675510; http://dx.doi.org/10.1371/journal.pone.0063853

9. Raven MA, Orton NC, Nassar H, Williams GA, Stell WK, Jacobs GH, Bech-Hansen NT, Reese BE. Early afferent signaling in the outer plexiform layer regulates development of horizontal cell morphology. J Comp Neurol 2008; 506:745-58; PMID:18076080; http://dx.doi.org/10.1002/cne.21526

10. tom Dieck S, Brandstätter JH. Ribbon synapses of the retina. Cell Tissue Res 2006; 326:339-46; PMID:16775698; http://dx.doi.org/10.1007/s00441-006-0234-0

11. Blanks JC, Adinolfi AM, Lolley RN. Synaptogenesis in the photoreceptor terminal of the mouse retina. J Comp Neurol 1974; 156:81-93; PMID:4836656; http://dx.doi.org/10.1002/cne.901560107

12. Regus-Leidig H, Tom Dieck S, Specht D, Meyer L, Brandstätter JH. Early steps in the assembly of photoreceptor ribbon synapses in the mouse retina: the involvement of precursor spheres. J Comp Neurol 2009; 512:814-24; PMID:19067356; http://dx.doi.org/10.1002/cne.21915

13. Taylor WR, Morgans C. Localization and properties of voltage-gated calcium channels in cone photoreceptors of Tupaia belangeri. Vis Neurosci 1998; 15:541-52; PMID:9685206; http://dx.doi.org/10.1017/S0952523898153142

14. Xu HP, Zhao JW, Yang XL. Expression of voltage-dependent calcium channel subunits in the rat retina. Neurosci Lett 2002; 329:297-300; PMID:12183035; http://dx.doi.org/10.1016/S0304-3940(02)00688-2

15. Specht D, Wu SB, Turner P, Dearden P, Koentgen F, Wolfrum U, Maw M, Brandstätter JH, tom Dieck S. Effects of presynaptic mutations on a postsynaptic Cacna1s calcium channel colocalized with mGluR6 at mouse photoreceptor ribbon synapses. Invest Ophthalmol Vis Sci 2009; 50:505-15; PMID:18952919; http://dx.doi.org/10.1167/iovs.08-2758

16. Schmitz F, Königstorfer A, Südhof TC. RIBEYE, a component of synaptic ribbons: a protein's journey through evolution provides insight into synaptic ribbon function. Neuron 2000; 28:857-72; PMID:11163272; http://dx.doi.org/10.1016/S0896-6273(00)00159-8

17. tom Dieck S, Altrock WD, Kessels MM, Qualmann B, Regus H, Brauner D, Fejtová A, Bracko O, Gundelfinger ED, Brandstätter JH. Molecular dissection of the photoreceptor ribbon synapse: physical interaction of Bassoon and RIBEYE is essential for the assembly of the ribbon complex. J Cell Biol 2005; 168:825-36; PMID:15728193; http://dx.doi.org/10.1083/jcb.200408157

18. Hack I, Frech M, Dick O, Peichl L, Brandstätter JH. Heterogeneous distribution of AMPA glutamate receptor subunits at the photoreceptor synapses of rodent retina. Eur J Neurosci 2001; 13:15-24; PMID:11135000; http://dx.doi.org/10.1046/j.1460-9568.2001.01357.x

19. Haeseleer F, Imanishi Y, Maeda T, Possin DE, Maeda A, Lee A, Rieke F, Palczewski K. Essential role of Ca^{2+}-binding protein 4, a Ca$_v$1.4 channel regulator, in photoreceptor synaptic function. Nat Neurosci 2004; 7:1079-87; PMID:15452577; http://dx.doi.org/10.1038/nn1320

20. Shaltiel L, Paparizos C, Fenske S, Hassan S, Gruner C, Rötzer K, Biel M, Wahl-Schott CA. Complex regulation of voltage-dependent activation and inactivation properties of voltage-gated L-type Ca^{2+} channels by Ca^{2+}-binding protein 4 (CaBP4). J Biol Chem 2012; 287:36312-21; PMID:22936811; http://dx.doi.org/10.1074/jbc.M112.392811

21. Maeda T, Lem J, Palczewski K, Haeseleer F. A critical role of CaBP4 in the cone synapse. Invest Ophthalmol Vis Sci 2005; 46:4320-7; PMID:16249514; http://dx.doi.org/10.1167/iovs.05-0478

22. Zeitz C, Kloeckener-Gruissem B, Forster U, Kohl S, Magyar I, Wissinger B, Mátyás G, Borruat FX, Schorderet DF, Zrenner E, et al. Mutations in CABP4, the gene encoding the Ca^{2+}-binding protein 4, cause autosomal recessive night blindness. Am J Hum Genet 2006; 79:657-67; PMID:16960802; http://dx.doi.org/10.1086/508067

23. Littink KW, van Genderen MM, Collin RW, Roosing S, de Brouwer AP, Riemslag FC, Venselaar H, Thiadens AA, Hoyng CB, Rohrschneider K, et al. A novel homozygous nonsense mutation in CABP4 causes congenital cone-rod synaptic disorder. Invest Ophthalmol Vis Sci 2009; 50:2344-50; PMID:19074807; http://dx.doi.org/10.1167/iovs.08-2553

24. Hemara-Wahanui A, Berjukow S, Hope CI, Dearden PK, Wu SB, Wilson-Wheeler J, Sharp DM, Lundon-Treweek P, Clover GM, Hoda JC, et al. A CACNA1F mutation identified in an X-linked retinal disorder shifts the voltage dependence of Ca$_v$1.4 channel activation. Proc Natl Acad Sci U S A 2005; 102:7553-8; PMID:15897456; http://dx.doi.org/10.1073/pnas.0501907102

25. Specht D, Tom Dieck S, Ammermüller J, Regus-Leidig H, Gundelfinger ED, Brandstätter JH. Structural and functional remodeling in the retina of a mouse with a photoreceptor synaptopathy: plasticity in the rod and degeneration in the cone system. Eur J Neurosci 2007; 26:2506-15; PMID:17970721; http://dx.doi.org/10.1111/j.1460-9568.2007.05886.x

26. Carter-Dawson LD, LaVail MM. Rods and cones in the mouse retina. I. Structural analysis using light and electron microscopy. J Comp Neurol 1979; 188:245-62; PMID:500858; http://dx.doi.org/10.1002/cne.901880204

27. Szél A, Röhlich P. Two cone types of rat retina detected by anti-visual pigment antibodies. Exp Eye Res 1992; 55:47-52; PMID:1397129; http://dx.doi.org/10.1016/0014-4835(92)90090-F

28. Morgans CW. Localization of the α($_{1F}$) calcium channel subunit in the rat retina. Invest Ophthalmol Vis Sci 2001; 42:2414-8; PMID:11527958

29. Xiao H, Chen X, Steele EC Jr. Abundant L-type calcium channel Ca$_v$1.3 (alpha1D) subunit mRNA is detected in rod photoreceptors of the mouse retina via in situ hybridization. Mol Vis 2007; 13:764-71; PMID:17563731

30. Busquet P, Nguyen NK, Schmid E, Tanimoto N, Seeliger MW, Ben-Yosef T, Mizuno F, Akopian A, Striessnig J, Singewald N. CaV1.3 L-type Ca2+ channels modulate depression-like behaviour in mice independent of deaf phenotype. Int J Neuropsychopharmacol 2010; 13:499-513; PMID:19664321; http://dx.doi.org/10.1017/S1461145709990368

31. Wu J, Marmorstein AD, Striessnig J, Peachey NS. Voltage-dependent calcium channel CaV1.3 subunits regulate the light peak of the electroretinogram. J Neurophysiol 2007; 97:3731-5; PMID:17376851; http://dx.doi.org/10.1152/jn.00146.2007

32. Baig SM, Koschak A, Lieb A, Gebhart M, Dafinger C, Nürnberg G, Ali A, Ahmad I, Sinnegger-Brauns MJ, Brandt N, et al. Loss of Ca($_v$)1.3 (CACNA1D) function in a human channelopathy with bradycardia and congenital deafness. Nat Neurosci 2011; 14:77-84; PMID:21131953; http://dx.doi.org/10.1038/nn.2694

33. Hope CI, Sharp DM, Hemara-Wahanui A, Sissingh JI, Lundon P, Mitchell EA, Maw MA, Clover GM. Clinical manifestations of a unique X-linked retinal disorder in a large New Zealand family with a novel mutation in CACNA1F, the gene responsible for CSNB2. Clin Experiment Ophthalmol 2005; 33:129-36; PMID:15807819; http://dx.doi.org/10.1111/j.1442-9071.2005.00987.x

34. Jacobi FK, Hamel CP, Arnaud B, Blin N, Broghammer M, Jacobi PC, Apfelstedt-Sylla E, Pusch CM. A novel CACNA1F mutation in a french family with the incomplete type of X-linked congenital stationary night blindness. Am J Ophthalmol 2003; 135:733-6; PMID:12719097; http://dx.doi.org/10.1016/S0002-9394(02)02109-8

35. Bradshaw K, Allen L, Trump D, Hardcastle A, George N, Moore A. A comparison of ERG abnormalities in XLRS and XLCSNB. Doc Ophthalmol 2004; 108:135-45; PMID:15455796; http://dx.doi.org/10.1023/B:DOOP.0000036786.22179.44

36. Xing W, Akopian A, Križaj D. Trafficking of presynaptic PMCA signaling complexes in mouse photoreceptors requires Cav1.4 α1 subunits. Adv Exp Med Biol 2012; 723:739-44; PMID:22183401; http://dx.doi.org/10.1007/978-1-4614-0631-0_94

37. Sheets L, Kindt KS, Nicolson T. Presynaptic CaV1.3 channels regulate synaptic ribbon size and are required for synaptic maintenance in sensory hair cells. J Neurosci 2012; 32:17273-86; PMID:23197719; http://dx.doi.org/10.1523/JNEUROSCI.3005-12.2012

38. LoGiudice L, Matthews G. The role of ribbons at sensory synapses. Neuroscientist 2009; 15:380-91; PMID:19264728; http://dx.doi.org/10.1177/1073858408331373

39. Dick O, tom Dieck S, Altrock WD, Ammermüller J, Weiler R, Garner CC, Gundelfinger ED, Brandstätter JH. The presynaptic active zone protein bassoon is essential for photoreceptor ribbon synapse formation in the retina. Neuron 2003; 37:775-86; PMID:12628168; http://dx.doi.org/10.1016/S0896-6273(03)00086-2

40. tom Dieck S, Specht D, Strenzke N, Hida Y, Krishnamoorthy V, Schmidt KF, Inoue E, Ishizaki H, Tanaka-Okamoto M, Miyoshi J, et al. Deletion of the presynaptic scaffold CAST reduces active zone size in rod photoreceptors and impairs visual processing. J Neurosci 2012; 32:12192-203; PMID:22933801; http://dx.doi.org/10.1523/JNEUROSCI.0752-12.2012

41. Aldahmesh MA, Al-Owain M, Alqahtani F, Hazzaa S, Alkuraya FS. A null mutation in CABP4 causes Leber's congenital amaurosis-like phenotype. Mol Vis 2010; 16:207-12; PMID:20157620

42. Bayley PR, Morgans CW. Rod bipolar cells and horizontal cells form displaced synaptic contacts with rods in the outer nuclear layer of the nob2 retina. J Comp Neurol 2007; 500:286-98; PMID:17111373; http://dx.doi.org/10.1002/cne.21188

43. Striessnig J, Bolz HJ, Koschak A. Channelopathies in Ca$_v$1.1, Ca$_v$1.3, and Ca$_v$1.4 voltage-gated L-type Ca^{2+} channels. Pflugers Arch 2010; 460:361-74; PMID:20213496; http://dx.doi.org/10.1007/s00424-010-0800-x

44. Doering CJ, Peloquin JB, McRory JE. The Ca($_v$)1.4 calcium channel: more than meets the eye. Channels (Austin) 2007; 1:3-10; PMID:19151588; http://dx.doi.org/10.4161/chan.3938

45. Gregory FD, Bryan KE, Pangršič T, Calin-Jageman IE, Moser T, Lee A. Harmonin inhibits presynaptic Cav1.3 Ca^{2+} channels in mouse inner hair cells. Nat Neurosci 2011; 14:1109-11; PMID:21822269; http://dx.doi.org/10.1038/nn.2895

46. Tippens AL, Pare J-F, Langwieser N, Moosmang S, Milner TA, Smith Y, Lee A. Ultrastructural evidence for pre – and postsynaptic localization of Ca$_v$1.2 L-type Ca^{2+} channels in the rat hippocampus. J Comp Neurol 2008; 506:569-83; PMID:18067152; http://dx.doi.org/10.1002/cne.21567

47. Herrmann R, Lobanova ES, Hammond T, Kessler C, Burns ME, Frishman LJ, Arshavsky VY. Phosducin regulates transmission at the photoreceptor-to-ON-bipolar cell synapse. J Neurosci 2010; 30:3239-53; PMID:20203183; http://dx.doi.org/10.1523/JNEUROSCI.4775-09.2010